Is a decline of AMOC causing the warming hole above the North Atlantic in observed and modeled warming patterns?

Sybren Drijfhout *
Geert Jan van Oldenborgh and Andrea Cimatoribus
Royal Netherlands Meteorological Institute, De Bilt, The Netherlands

ABSTRACT

The pattern of Global Mean Temperature (GMT) change is calculated by regressing local Surface Air Temperature (SAT) to GMT for an ensemble of CMIP5 models and for observations over the last 132 years. Calculations are based on the historical period and climate change scenarios. As in the observations the warming-pattern contains a warming hole over the subpolar North Atlantic. Using a bivariate regression of SAT to GMT and an index of the Atlantic meridional overturning circulation (AMOC), the warming-pattern is decomposed in a radiatively forced part and an AMOC fingerprint. The North Atlantic warming hole is associated with a decline of the AMOC. The AMOC fingerprint resembles Atlantic Multidecadal Variability (AMV), but details of the pattern change when the AMOC decline increases, underscoring the non-linearity in the response.
The warming hole is situated south of deep convection sites, indicating that it involves an adjustment of the gyre circulation, although it should be noted that some models feature deep convection in the middle of the subpolar gyre. The warming hole is already prominent in historical runs, where the response of the AMOC to GMT is weak, which suggests that it is involved in an ocean adjustment that precedes the AMOC decline. In the more strongly forced scenario runs, the warming hole over the subpolar gyre becomes weaker, while cooling over the Nordic Seas increases, consistent with previous findings that deep convection in the Labrador and Irminger Seas is more vulnerable to changes in external forcing than convection in the Nordic Seas, which only reacts after a threshold is passed.

1. Introduction

In climate change scenarios the AMOC is projected to weaken during the 21^{st} century in response to enhanced greenhouse gas forcing (**?**). The associated cooling is expected to partly offset the greenhouse-induced warming in SAT over the North Atlantic. **?** show that a larger reduction in the AMOC is associated with greater cooling in the North Atlantic (their Figure 1). Although the cooling features a marked spatial pattern, its uniform sign north of 20°N suggests that the response to an AMOC-decline projects on AMV (**?**), underscoring the hypothesis that AMV is for a large part driven by AMOC changes (**??**). For instance, the correlation between AMOC and AMV on multidecadal to centennial timescales can exceed 0.8 in a coupled climate model (**?**).

This implies that the AMV is not only the dominant pattern of observed detrended 20^{th} century multidecadal SST-anomalies; it also would project on the warming-pattern of anthropogenically forced SAT insofar a forced decline of the AMOC is involved. A calculation of the warming pattern of GMT, by regressing observed SAT to GMT, reveals that at most places SAT and GMT are positively correlated. At some places, however, a negative regression coefficient arises, noticeably over the North Atlantic and North Pacific subpolar gyres. When the data are smoothed over decadal timescales, the negative regression over the North Atlantic becomes more prominent, while the area with negative regression coefficients over the North Pacific declines, suggesting different physical mechanisms at work. An increase of the cooling over the North Atlantic when timescale increases is consistent with the hypothesis that the North Atlantic warming hole is associated with AMOC decline: the anthropogenically forced signals of AMOC decline and GMT rise correlate well, while the shorter-time natural fluctuations in AMOC and GMT don't. Figure 1a shows the regression of SAT on GMT for the observations in the North Atlantic sector after applying a decadal low-pass filter, highlighting the warming hole over the subpolar gyre.

In the following we show that the CMIP5 model ensemble features a similar North Atlantic warming hole in climate change scenarios and historical runs. In each scenario, the warming hole can be linked to a decline of the

AMOC, but the fingerprint of AMOC decline changes for scenarios featuring stronger radiative forcing. In these scenarios cooling over the Nordic Seas becomes more prominent. This paper is organized as follows. In Section 2, we describe the data and the methodology used in this study. The results of the regression analysis are presented in Section 3. Section 4 summarizes the main results.

2. Data and methodology

Climate model simulations from the World Climate Research programme's Coupled Model Intercomparison Project phase 5 (CMIP5) (**?**) have been used and compared to observations from the GISTEMP-1200 dataset (**?**). For the CMIP5 analysis we used the historical runs, representing the late 19^{th} and 20^{th} century, and the RCP2.6, RCP4.5 and RCP8.5 scenarios for the 21^{st} century. Apart from SAT, meridional overturning streamfunction data were used. From these, an AMOC index was calculated by averaging the AMOC-strength between 500 and 2000 m depth and between the southern boundary of the Atlantic, around 34°S, and 50°N. In this way an index is obtained that optimally reflects large-scale changes in the AMOC associated with a long-term, anthropogenically forced trend, which indeed has a basin-scale expression (**?**). At the same time the expression of natural AMOC variability is minimized, which is often characterized by a dipole-pattern with a maximum amplitude near the AMOC maximum, see e.g. **?** and **?** for a discussion of the relevant patterns.

The total number of models used is 12 (Table 1), determined by the availability of meridional overturning streamfunction data for the RCP2.6 scenario, which is less frequently simulated. The scenario runs and historical period were joined together, creating timeseries of 240–251 years long. The period after 2100 was excluded, to prevent one model getting to a high weight when the ensemble-mean is calculated. Also, only one ensemble-member was used for each model. In addition, the historical period was treated separately. For all models a univariate regression of SAT on GMT was performed by a simultaneous regression of all modeled SAT-fields on GMT. That is, timeseries of all models were joined:

$$T(x,y,t,i) = A(x,y)T_{\text{global}}(t,i) + \varepsilon(x,y,t,i), \qquad (1)$$

with $i = 1 \ldots N$ an index over the different models and $A(x,y)$ the warming-pattern.

Also, a bivariate regression of SAT on both GMT and the AMOC-index was carried-out:

$$T(x,y,t,i) = B(x,y)T_{\text{global}}(t,i) + C(x,y)\Psi(t,i) + \varepsilon(x,y,t,i), \qquad (2)$$

with $B(x,y)$ the radiatively forced pattern, $C(x,y)$ the AMOC fingerprint, and Ψ the AMOC-index.

We performed lagged-regressions as well, because the response of SAT to AMOC-variations is not instantaneous (**?**), but since a variety of timescales is involved, all being model dependent, we discarded lagged-regressions, as the regressions with zero lag generally gave the best results. Before performing the regression, at each point and in each model the time-averaged temperature and AMOC-index was subtracted. The regression on the anomalies was performed with standard R routines.

3. Regression patterns

The models' pattern of GMT change is shown in Fig. 1b, c, d, for the historical period; the RCP2.6 scenario; and the RCP8.5 scenario. All warming-patterns show a similar warming hole over the North Atlantic as for the observations (Fig. 1a), but the warming hole becomes less prominent when the radiative forcing gets stronger. It is most prominent in the historical run, and most weak in the RCP8.5 scenario. If the warming hole would be caused by a decline of the AMOC, this suggests that the sensitivity of the AMOC for GMT change becomes weaker in a warmer climate. This is corroborated by the decreased regression of AMOC on GMT in more strongly forced scenarios, although the decrease is not significant (Table 1). Figure 1 also shows that the warming hole is larger in the observations than in the model ensembles.

By performing a bivariate regression, the pattern of GMT change can be decomposed into a pattern that is associated with the radiative forcing (assuming that this drives the GMT change in the RCP scenarios) and the fingerprint of the AMOC on SAT. Figure 2 shows that in the historical run the radiatively forced part still features a somewhat weaker warming hole, but in the RCP2.6 and other scenarios the warming hole is absent in the radiatively forced pattern. There, it is completely attributed to the AMOC fingerprint. This fingerprint has a roughly similar pattern as AMV, with warming over the North Atlantic associated with a positive AMOC anomaly (Figs. 2b, d). This result corroborates the hypothesis that the warming hole in the GMT trend-pattern is caused by a decline of the AMOC.

At first sight, it may seem surprising that the warming hole is still part of the radiatively forced pattern in the historical runs. This could suggest that the separation between the radiatively forced pattern and the AMOC fingerprint is still incomplete. However, since the response of the AMOC to GMT is small in the historical runs (Table 1) and GMT and AMOC are more weakly correlated than in the scenario runs (Table 2), a separation between the two patterns should work well for the historical runs. There must be another reason why the warming hole is less well associated with the AMOC in the historical runs. Several conjectures can be made to explain what is going on. One hypothesis is that the warming hole is part of an ocean adjustment that already precedes AMOC decline. In par-

ticular, in the RCP2.6 scenario the correlation between the warming hole and the AMOC increases, compared to the historical run, while the correlation between the warming hole and GMT becomes less negative (Table 2). This corroborates the hypothesis that the warming hole is partly forcing a lagged AMOC response. In the more strongly forced scenarios the correlation between the warming hole and both GMT and AMOC increase further, as they both are dominated by a large, monotonic trend. Note that these results do not change qualitatively when the AMOC-index is derived from the maximum overturning, only the amplitude of the AMOC fingerprint is weaker in that case.

A second conjecture is that aerosols partly cause the warming hole in the historical runs. Since they have a stronger influence on the 20^{th} century climate than on future projections, the warming hole could be part of the radiatively-forced pattern in historical runs, while in the scenario runs it would be due to the AMOC. Whether aerosols do play a role in producing the North Atlantic warming hole remains unclear. For instance, **?** found cooling over the midlatitude North Pacific due to aerosols, but found a weak, diffusive signal over the North Atlantic. On the other hand, **?** suggest a strong link between aerosols and the AMV. While there are too many unknowns in the historical aerosol forcing to unequivocally attribute SAT-fingerprints to aerosol forcing, the possibility that aerosol forcing might be partly responsible for the warming hole in the historical period cannot be excluded.

A third conjecture is that the main driver for AMOC variability changes between the historical period and future scenarios. In the historical runs a lot of AMOC variations may be associated with wind stress changes, while in the scenario runs the change in hydrological cycle might become the dominant driver for AMOC changes.

The warming hole is situated southeast of the deep convection sites in the Labrador and Irminger Sea, indicating that it cannot be interpreted as the passive SAT-response to changes in deep convection. It must also involve changes in the subpolar gyre circulation, which would point to conjecture one. On the other hand, many climate models feature deep convection west of Ireland, associated with a too zonal North Atlantic Current (**?**). However, both in the observations and in the CMIP3 ensemble the warming hole is situated south of the regions of maximum heat loss (**?**), suggesting that it does not arise as a passive response to a decrease in deep convection.

The decrease of the warming hole for more strongly forced scenarios is not simply the expression for a decreased sensitivity of the AMOC to further GMT rise after GMT has increased. Although the regression of AMOC strength per degree GMT slightly changes, decreasing from the RCP2.6 to the RCP8.5 scenarios (Table 1), the decrease is not significant. An inspection of the differences between the patterns for the various scenarios reveals that the more strongly forced scenarios feature larger cooling in the Nordic Seas (Fig. 3). This can be explained by the fact that in most models convection in the Labrador and Irminger Seas is more vulnerable to changes in external forcing, and that in general the Labrador and Irminger Seas first respond to climate change, only followed by the Nordic Seas when convection in the Labrador and Irminger Seas have nearly ceased (**???**). So, although the warming hole is not situated above the regions of maximum heat loss, there must be a link between the warming hole and changes in deep convection in the western part of the subpolar North Atlantic.

4. Summary and Conclusions

We have investigated the GMT trend-pattern in the observations and in CMIP5 models. The pattern was decomposed in a radiatively forced part and an AMOC fingerprint. The trend-pattern obtained by regressing SAT on GMT contains a warming hole over the subpolar North Atlantic. By use of a bivariate regression we were able to demonstrate that the warming hole is associated with the AMOC; in the RCP scenarios the radiatively forced fingerprint does not contain the warming hole. The AMOC fingerprint in the RCP scenarios resembles the AMV, (**???**), corroborating the finding of **?** that phasing of the AMV can be paced by the external forcing, although details of the fingerprint change when forcing and AMOC-decline become stronger.

The warming hole is situated southeast of the deep convection sites in the Labrador and Irminger Seas, which is once more a sign of the complex relation between convective overturning and the AMOC (**??**). The fact that both observations and models show maximum cooling in the center of the subpolar gyre indicates that both subpolar gyre and AMOC adjust in concert, but with different time lags; a feature that has been discussed in various modeling studies (**??**). A lagged adjustment to global warming of the AMOC, preceded by a adjustment of the subpolar gyre, is consistent with the warming hole being most prominent in the historical runs, where the AMOC decline per degree GMT is smallest. Other conjectures, however, also offer explanations for this feature. In the RCP scenarios the model ensemble captures an AMOC fingerprint that elucidates the observed warming hole, which is absent in the radiatively forced pattern. This strong connection is apparent in all scenarios where the AMOC is dominated by a downward trend. Model spread in fingerprint and response of the AMOC to GMT, however, is very large, underscoring the large uncertainty in AMOC projections for the next century (**?**). When the radiative forcing becomes stronger, a robust increase of cooling over the Nordic Seas arises, which is consistent with previous findings that deep convection in the Labrador and Irminger Seas is more vulnerable

to changes in external forcing, and that the convection in the Nordic Seas only reacts to changes in external forcing after a threshold is passed, underscoring the non-linearity of the AMOC response.

AMOC fingerprints in other measures than SAT have been promoted by **?** and **?**. It remains a challenge to investigate whether their fingerprints can be recovered from the CMIP5 ensemble applying the same technique as used here. Establishing the relation between the AMOC fingerprint on SAT, and other quantities, such as sea surface height, subsurface temperature and upper ocean heat content, would enable a more dynamical understanding of how the subpolar warming hole arises in association with an AMOC decline.

Finally, we address whether the question posed in the title of this manuscript has been answered. With the present knowledge, we point to the case that all model results indicate that the warming hole is the precursor of an AMOC decline that is bound to occur in the coming century.

Acknowledgments.

We acknowledge the World Climate Research Programme's Working Group on Coupled Modelling, which is responsible for CMIP, and we thank the climate modeling groups for producing and making available their model output. For CMIP5 the U.S. department of Energy's Program for Climate Model Diagnosis and Intercomparison (PCMDI) provides coordinating support and led development of software infrastructure in partnership with the Global Organization for Earth System Science Portals. In particular, we thank ETHZ for making possible to download CMIP5 data from their server. We acknowledge the editor and two anonymous referees for their constructive comments.

TABLE 1. The regression of the AMOC-index on GMT in $10^6\,m^3\,s^{-1}\,K^{-1}$ for the 12 models of CMIP5 that were analysed

Model	*historical*	*RCP*2.6	*RCP*4.5	*RCP*8.5
CanESM2	0.60	-0.80	-0.78	-0.72
CCSM4	-0.90	-1.44	-1.51	-1.52
CESM1-CAM5	-0.05	-2.23	-2.14	-1.81
CNRM-CM5	-0.98	-1.47	-1.24	-1.02
FGOALS-g2	0.35	-2.76	-2.16	-1.54
FGOALS-s2	-1.00	-3.00	-2.86	-2.03
GFDL-CM3	0.63	-2.84	-2.48	-2.11
GFDL-ESM2M	-1.37	-3.15	-3.13	-2.80
MPI-ESM-LR	-0.48	-1.53	-1.46	-1.17
MPI-ESM-MR	0.31	-1.03	-1.11	-1.00
MRI-CGCM3	-0.04	-0.88	-0.74	-0.92
NorESM1-M	0.89	-1.78	-1.88	-1.94
Ensemble Mean	-0.4±0.8	-1.9±0.8	-1.8±0.8	-1.5±0.6

TABLE 2. The correlation between GMT and the AMOC-index; the warming hole and the AMOC-index; and the warming hole and GMT for the CMIP5 model ensemble. The warming hole is defined as temperature averaged over 40°W and 20°W, and 45°N and 60°N minus temperature averaged over 45°N and 60°N. In this calculation the RCP scenarios were taken separately, not joined with data from the historical period

Scenario	*AMOC/GMT*	*AMOC/WH*	*GMT/WH*
historical	-0.16	0.23	-0.50
RCP2.6	-0.61	0.57	-0.41
RCP4.5	-0.79	0.71	-0.67
RCP8.5	-0.90	0.87	-0.85

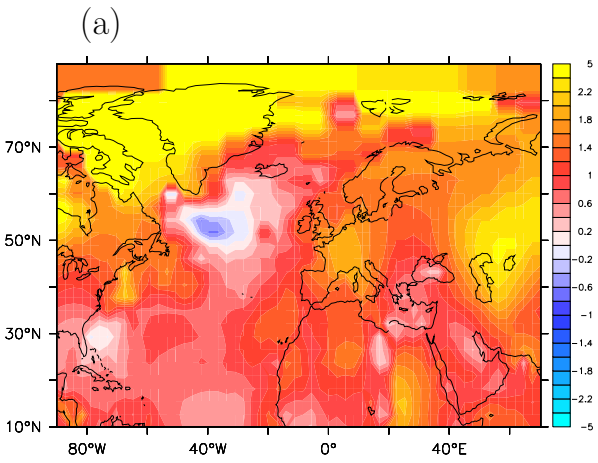

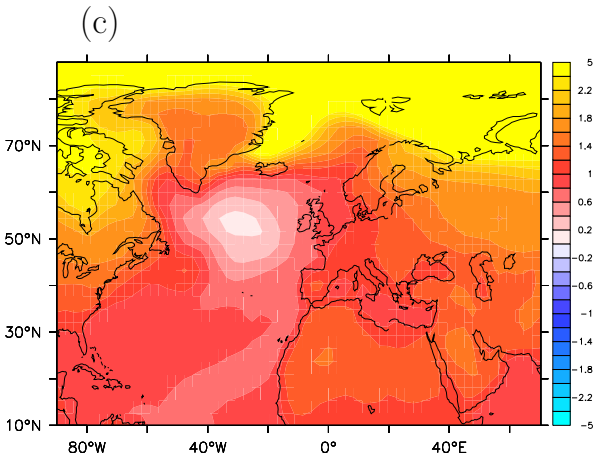

Fig. 1. Trend-pattern of GMT in the North Atlantic sector, obtained by a univariate regression of SAT on GMT, for a) observations; b) historical runs; c) the RCP 2.6 scenario; d) the RCP8.5 scenario

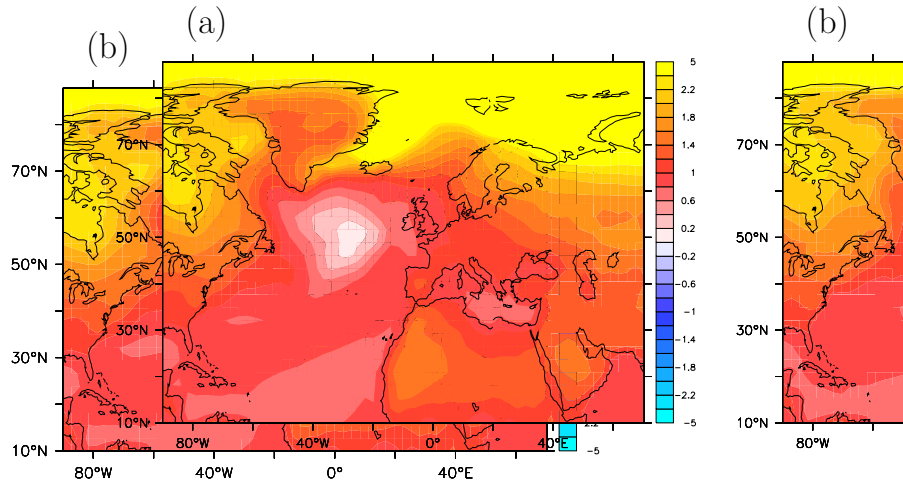

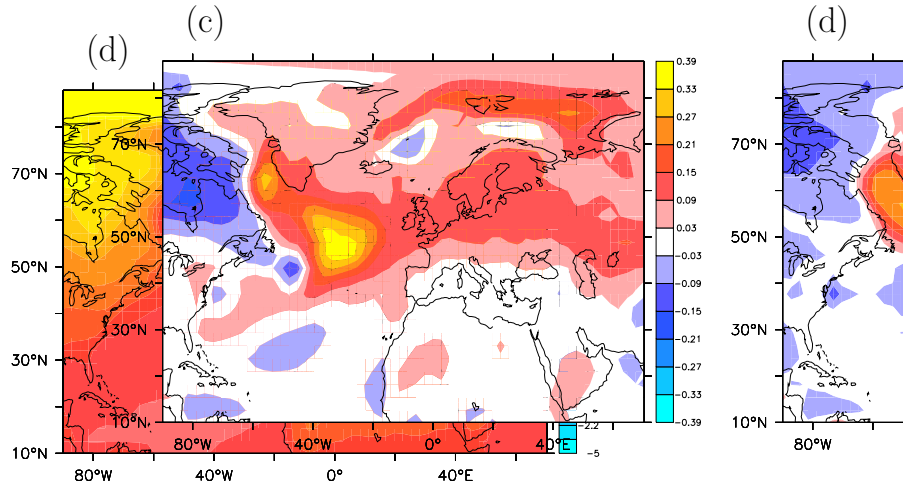

Fig. 2. Fingerprints obtained by a bivariate regression of SAT on GMT and an AMOC index, for a) radiative forcing fingerprint in the historical run; b) radiative forcing fingerprint in the RCP2.6 scenario; c) AMOC fingerprint in the historical run; d) AMOC fingerprint in the RCP2.6 scenario

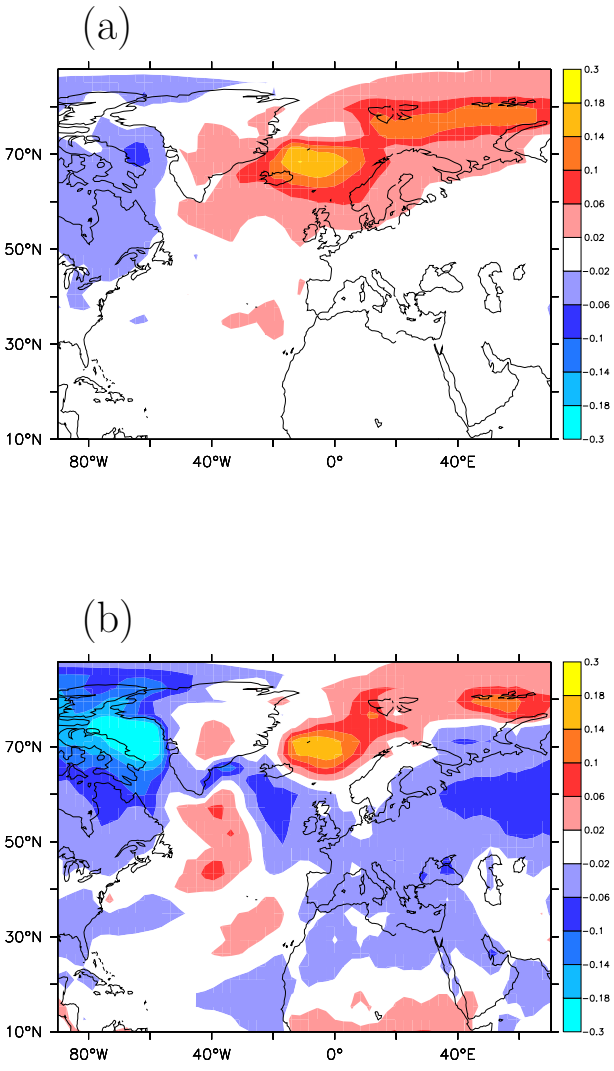

FIG. 3. Difference in AMOC fingerprints for a) RCP4.5 minus RCP2.6 scenario; b) RCP8.5 minus RCP2.6 scenario